

Synthesis of ZnO-based varistor precursor powders by means of the reaction spray process

O. MILOŠEVIĆ, D. USKOKOVIĆ

Institute of Technical Sciences of the Serbian Academy of Sciences and Arts, Belgrade, Yugoslavia PO Box 745

L. J. KARANOVIĆ

Faculty of Mining and Geology, Belgrade, Yugoslavia

M. TOMAŠEVIĆ-ČANOVIĆ

Institute for Technology for Nuclear and other Mineral Raw Materials, Belgrade, Yugoslavia

M. TRONTELJ

Jožef Štefan Institute, Ljubljana, Slovenia

High-purity, fine-grained oxide ceramic powders that are commonly used for ZnO-based varistors were synthesized by means of the reaction spray process. Processing steps included formation of the solutions of zinc nitrate and/or certain metal additives and spraying of the solution into a heated reaction column using a two-phase nozzle. After water evaporation from the droplets, the precursor salts were decomposed at elevated temperatures (up to 1473 K) in order to obtain homogeneous oxide powders with complex compositions corresponding to the final multicomponent varistor system. The decomposition behaviour of the precursors, as well as the characteristics of the resulting powders: crystallinity, phase composition, particle shape, morphology and particle-size distribution, were examined. It was shown that the characteristics of the reaction spray-derived powders can be controlled by adjusting the system and the solutions parameters.

1. Introduction

The preparation of ceramic materials with a high degree of compositional and microstructural homogeneity, high purity and reliability is based on the capability of generating fine powders, often of unstable or metastable phases with a narrow distribution of particle sizes and a small mean size. The application of wet chemical techniques, including homogeneous precipitation, sol-gel, gas-phase reactions, etc., to the formation of ceramic materials is based on a number of important characteristics and has frequently been mentioned as more advantageous as compared to conventional methods [1–3]. However, it is often difficult to obtain chemically homogeneous oxide powder with a complex composition by solution techniques, due to the imperfect coprecipitation resulting in variation of composition of each precipitated particle.

The reaction spray process (evaporative decomposition of solution; spray pyrolysis) is one of the dispersion phase techniques and it is recognized as an important method for making fine powders and materials, e.g. homogeneous mixtures CaO–Al₂O₃ [3], compounds MgO, Al₂O₃, MgAl₂O₄, MgCr₂O₄ [4],

ZnO [5], precursor powders for sulphide ceramics [6], precursor powders for electronic ceramics [7, 8], superconducting fine particles in the Bi–(Pb)–Ca–Sr–Cu–O system [9], ZrSiO₄ microspheres [10], fine spherical yttria-stabilized zirconia [11, 12], PLZT [13] and V₂O₃ [14] fine powders, etc.

It involves atomizing the solution into a heated reaction column. The mist of the solution is dried and subsequently decomposed at elevated temperatures. This permits higher surface reaction and prevents any compositional segregation. Therefore, this method is considered to produce powders maintaining compositional homogeneity and to have the advantage of ease of close compositional control for the multicomponent powders.

When materials and devices for electronics are considered (e.g. multicomponent ZnO-based non-linear resistors (varistors)), a high degree of homogeneity, controlled and/or fine-grain size and controlled grains and grain-boundary chemistry are important and critical for performance. Therefore, it has been shown that a higher activity of chemically prepared varistor precursor powders enables one to obtain the fine-grained ceramics with improved electrical properties [15].

The purpose of this work was to develop the equipment and the method for the production of multicomponent ZnO-based varistor precursor powders with controlled characteristics by means of the reaction spray process. In this context, the investigation results for a one-component ZnO-based model system, as well as for the system (ZnO + additives), will be presented.

2. Experimental procedure

2.1. Laboratory equipment for the reaction spray process

The main parts of the equipment are: (i) an atomizing system, including a twin-fluid atomizer, which was used in this work; an ultrasonic atomizer, Gapusol 9001 type, 2.5 MHz, RBI is also available; (ii) a vertical tube furnace (Electron-Ignis Combo Lab.) height 1750 mm with plasma-generated alumina tube 150 mm diameter with three independently controllable temperature zones, each of 1473 K maximum; a microcomputer-based temperature-indicated controller MCM-100 series (Shinko) and AR-201 six-point Toshiba recorder.

The general process flow diagram of the reaction spray process for the production of ceramic powders is shown in Fig. 1. The solution of metal salts was atomized into a hot reaction column, where the droplets were dried and decomposed in a dispersed phase. To cause a gas-liquid (droplets) dispersed system flow through the furnace, a pressure drop was maintained at the exhaust by means of a vacuum pump. Separation of the gas-borne particles from the gas stream (mixture of gases and water vapour) was achieved by deposition on collecting surfaces in gravity settling chambers. The process parameters, the gas and the

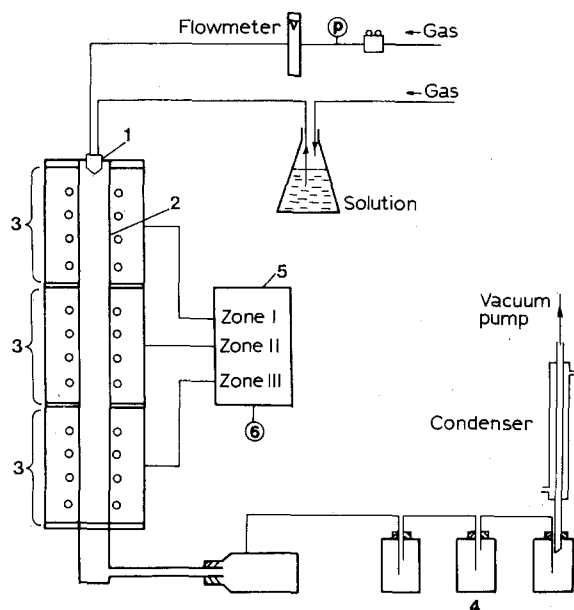


Figure 1 A laboratory system for the powder preparation by the reaction spray process. 1, Twin-fluid atomizer; 2, alumina tube (diameter 160 mm, $l = 1770$ mm); 3, furnace (Electron-Ignis Combo Lab.); 4, gravity settling chambers; 5, micro-computer-based temperature-indicating controller MCM-100 series (Shinko); 6, AR 201 six-point recorder (Toshiba).

liquid flow rates and the temperatures in the reaction zones were adjusted initially.

2.2. Preparation of ZnO powders by means of the reaction spray process

The feed solution was a water-soluble salt α -Zn(NO₃)₂·6H₂O (Merck, p.a.) dissolved in distilled water at room temperature in proportions to obtain 1M solution of zinc nitrate which was used in all experiments. Nitrogen gas was used as an atomizing medium. The gas pressure was maintained at 0.5 bar and the liquid flow rate was 0.6 l h⁻¹. The feed solution was fed to an atomizing system, sprayed and decomposed into a reaction column. The temperature profiles in the reaction column zones are given in Table I. After spraying and decomposition, powder 0.22_r was exposed to flowing hot gases at the exhaust for about 30 min.

Note that an initial α -Zn(NO₃)₂·6H₂O was also decomposed for comparison by means of conventional decomposition in a tube furnace (Heraeus, ROF 7/50) at 573 K for 2 h.

2.3. Preparation of multicomponent ZnO-based varistor precursor powder by means of the reaction spray process

In order to obtain powder with complex initial composition (100-X)ZnO + Y(additives), the following starting components were used: Zn(NO₃)₂·6H₂O (Merck extra pure), Bi(NO₃)₃·9H₂O (Kemika, p.a.), SbCl₃ (Kemika, 99%), Co(NO₃)₂·6H₂O (Merck, p.a.), Mn(CH₃COO)₂·4H₂O (Merck, extra pure), Cr(NO₃)₃·9H₂O (Merck, p.a.) and Ni(NO₃)₂·6H₂O (Merck, p.a.).

The starting components were dry mixed and heated to form a homogeneous common grey solution [16]. The solution obtained was diluted with distilled water in the proportions of the desired composition and mixed thoroughly. The suspension thus obtained was fed to an atomizing system and sprayed into a reaction column. The gas pressure (nitrogen) was 0.5 bar, the liquid flow rate was 0.5 l h⁻¹ and the temperature profiles in the reaction column zones were as given in Table I (powder 0.24). After spraying and decomposition of the complete suspension, the resulting powder was exposed to flowing hot gases at the exhaust for about 30 min.

TABLE I The temperature profiles in the zones of the reaction column during the reaction spray process

No.	Temperature, (K)			Feed solution
	Zone I	Zone II	Zone III	
0.21	473	873	873	α -Zn(NO ₃) ₂ ·6H ₂ O
0.22	473	1073	1073	
0.22 _r	473	1073	1073	
0.23	473	1173	1173	
0.24	473	1173	1173	α -Zn(NO ₃) ₂ ·6H ₂ O + additives

Powder 0.24 was compacted into samples having a diameter of 8 mm and a height of 1–2 mm at a uni-axial pressing pressure of 80 MPa. The samples were sintered in air from 1373–1573 K, held for 60 min; heating and cooling rates were controlled at 5 K min⁻¹.

2.4. Characterization

The development of the crystal phases in powders was studied with a Philips PW 1710 diffractometer using a graphite-monochromatized CuK_α radiation. DTA and TGA were performed in air at heating rates of 10 K min⁻¹ (Netzch 409 EP). The powder-size distribution was performed using Coulter Multisizer. Powder morphology was examined by SEM (AMR-1600 T). The chemical homogeneity of the microstructures was determined by EDS (PGT system IV from Princeton Gamma Tech.).

Electrical measurements were registered within the interval 1–100 A m⁻² by a d.c. power supply. The non-linearity coefficients were determined within the range from 1–10 A m⁻² (α_1) and 10–100 A m⁻² (α_2); the breakdown field, K_c , was determined at 10 A m⁻² and the leakage current, J_L , was measured at a voltage of 0.8 K_c .

3. Results and discussion

3.1. Thermal analysis

The thermal analysis results for Zn(NO₃)₂ · 6H₂O and for powders obtained in accordance to Table I, heated at 10 K min⁻¹ in air, are presented in Fig. 2. The zinc nitrate decomposition can be divided into dehydration processes for temperatures up to 473 K (multiple stage endothermic reaction with the peak temperature of 324 and 374 K), and decomposition up to 623 K, in agreement with the literature data [17]. Maximum weight loss is 76% up to 633 K (Fig. 2a). From the thermal analysis, it can be concluded that the zinc nitrate salt is an acceptable precursor material for powder synthesis by the reaction spray process, because full decomposition can be achieved at reasonably low temperatures (up to 633 K). Bearing in mind that the effective heating rate of a salt droplet/particle during the reaction spray process is approximately 300 K s⁻¹ [17], the low-temperature decomposition salts are preferable.

The decomposition curves for powder obtained by reaction spraying of zinc nitrate solution at 1073 K (powder 0.22) indicated the presence of unreacted phases up to 573 K with a maximum weight loss of 28% (Fig. 2b). The relative degree of decomposition, δ , was determined from TGA and calculated from the relation [18]

$$\delta = W_F/W_A \quad (1)$$

where W_F is the final sample weight after complete decomposition and W_A is the sample weight after the loss of adsorbed water. For powder 0.22, $\delta = 0.81$.

When hot gases flow over as-prepared powder in the exhaust for a certain period of time (powder 0.22_f),

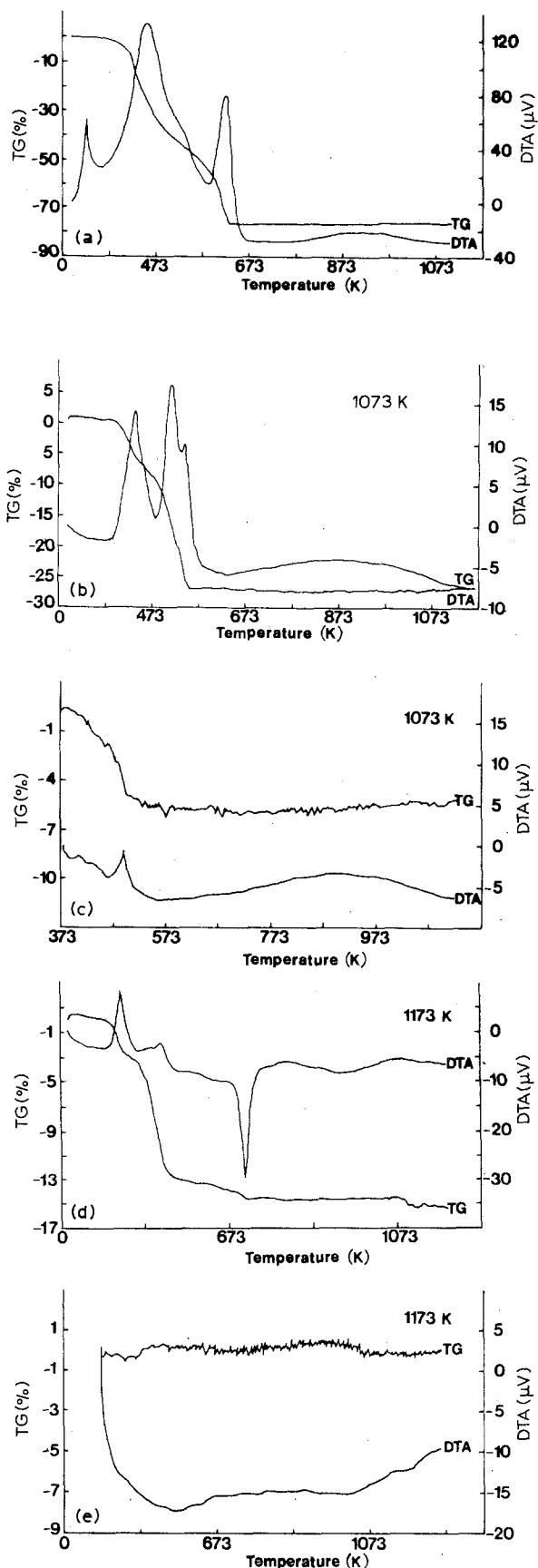


Figure 2 Thermal analysis results (a) for Zn(NO₃)₂ · 6H₂O, and for powder decomposed by means of the reaction spray process: (b, c) 0.22, (d) 0.23 and (e) 0.24, heated at 10 min⁻¹ in air.

thermal decomposition curves presented in Fig. 2c indicate that the decomposition is complete and $\delta = 1$. This implies that adsorption of water vapour is prevented.

At the reaction temperature of 1173 K (powder 0.23), the thermal analysis indicated that the decomposition of the obtained powder is completed up to 573 K and $\delta = 0.9$. This indicates that the small amount of a residual unreacted phase is presented in the sample. Note that an exothermic peak is evident at 673 K because little weight loss is observed (Fig. 2d).

The decomposition curves for powder obtained by the reaction spraying of (the zinc nitrate + additives) water suspension at 1173 K (Fig. 2e) show complete decomposition with $\delta = 1$.

3.2. Powder characteristics

The effect of the reaction spray process temperature on the crystallinity of the zinc nitrate derived powders is shown in Fig. 3. At a reaction temperature of 873 K (0.21) the decomposition is not completed. Poorly crystalline ZnO as well as $\text{Zn}_5(\text{NO}_3)_2(\text{OH})_8 \cdot 2\text{H}_2\text{O}$ as dominant phases are found in the sample. The formation of the intermediate phase $\text{Zn}_5(\text{NO}_3)_2(\text{OH})_8 \cdot 2\text{H}_2\text{O}$ is a result of the rehydration of the partially decomposed anhydrous salt by adsorption of water vapour from the exhaust gas [18]. As the reaction temperature is further increased to 1073 K (powder 0.22) the content of ZnO phase is also increased. At a reaction temperature of 1173 K (powder 0.23) the X-ray diffraction (XRD) yielded crystalline ZnO as a dominant phase and a few poor peaks of an intermediate phase $\text{Zn}_5(\text{NO}_3)_2(\text{OH})_8 \cdot 2\text{H}_2\text{O}$. The ratio R , between the intensity of the ZnO (100) peak at 31.7° (2θ) versus the intensity of the $\text{Zn}_5(\text{NO}_3)_2(\text{OH})_8 \cdot 2\text{H}_2\text{O}$ (200) peak at 9.1° (2θ) increases with

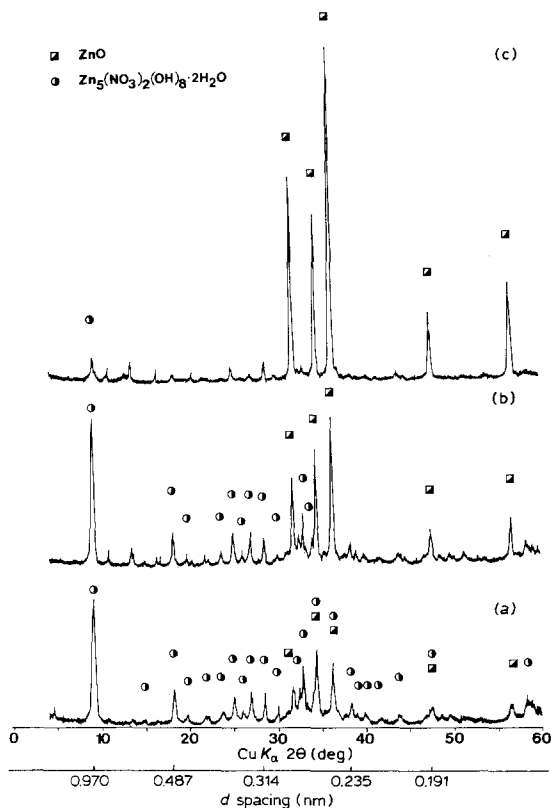


Figure 3 XRD patterns for zinc nitrate decomposed by the reaction spray process at (a) 873, (b) 1073 and (c) 1173 K.

the reaction spray temperature as the extent of decomposition of the nitrate precursor increases (Fig. 4).

The XRD patterns of the zinc nitrate and (the zinc nitrate + additives), decomposed by means of the reaction spray process at 1073 and 1173 K, respectively, when exposed to flowing hot gases at the exhaust, are presented in Fig. 5. When zinc nitrate is decomposed conventionally in static conditions, the full decomposition is achieved at 573 K for 2 h and the XRD yielded the powder pattern of hexagonal ZnO.

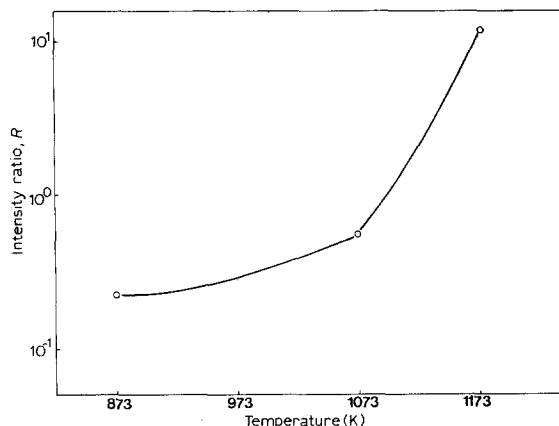


Figure 4 The ratio R between the intensity of the ZnO (100) peak at 31.7° (2θ) versus the intensity of the $\text{Zn}_5(\text{NO}_3)_2(\text{OH})_8 \cdot 2\text{H}_2\text{O}$ (200) peak at 9.1° (2θ) as a function of nominal reaction spray temperatures.

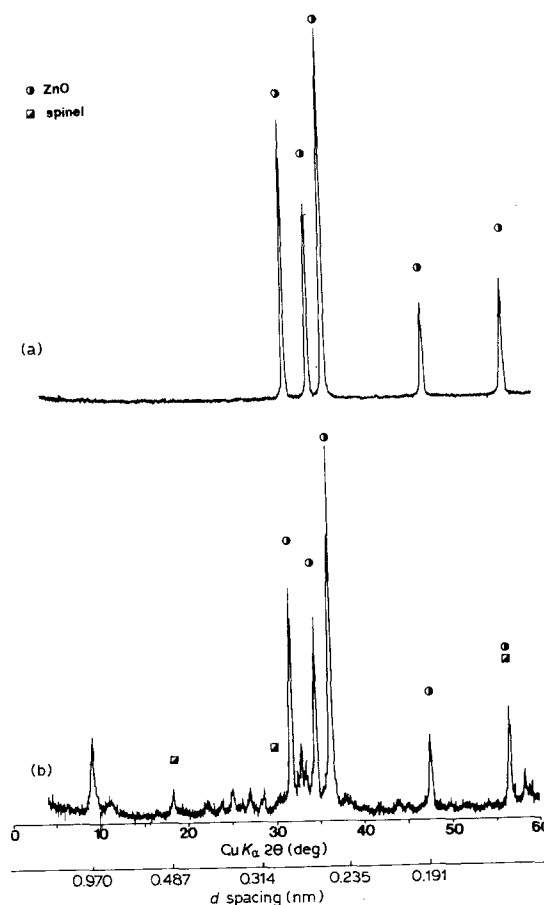


Figure 5 X-ray powder patterns for (a) $\text{Zn}(\text{NO}_3)_2 \cdot 6\text{H}_2\text{O}$, and (b) $\text{Zn}(\text{NO}_3)_2 \cdot 6\text{H}_2\text{O}$ + additives, decomposed by the reaction spray process at 1073 and 1173 K, respectively, when exposed to flowing hot gases at the exhaust.

For powder 0.22_r, exposed to flowing hot gases in the exhaust, the XRD implies only the presence of ZnO phase in the resulting powder (Fig. 5a). In the case of samples obtained by the reaction spray decomposition of zinc nitrate + additives suspension, the presence of well-crystallized ZnO phase, as well as poorly crystallized spinel phase, is evident. Diffraction maxima at 0.375, 0.227, 0.255 and 0.2031 nm are not clearly identified (Fig. 5b).

The results of particle-size distribution of powders 0.21–0.24 are plotted as particle diameters against cumulative weight undersize on logarithm probability papers (Fig. 6). The near linearity observed for all powders examined implies that the distribution may be approximated by log-normal distribution. The mean particle sizes, D_{50} , were graphically determined for each distribution and are also presented in Fig. 6. It is evident that the increasing temperature of the reaction spray process did not affect the mean particle size.

Scanning electron micrographs of the zinc nitrate-derived powders prepared conventionally and according to the reaction spray process at 873–1173 K are presented in Fig. 7. The particles are almost spherical, although there is some content of irregularly shaped

particles. As previously predicted [8], the particles obtained are hollow spherical shells and shell fragments. The particle surfaces are not smooth. Each particle seems to be an aggregate of small individual particles which are $\leq 1 \mu\text{m}$ diameter.

EDS analysis for powder 0.24 (zinc nitrate + additives) are presented in Fig. 8a for particle surfaces and for the bulk. In both cases the presence of zinc is clearly visible, together with other elements such as

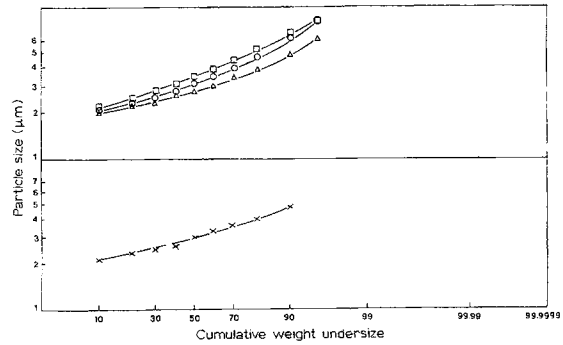


Figure 6 Log-probability plot of powders 0.21–0.24. D_{50} (μm): (○) 3.16, powder 0.21; (□) 3.56, powder 0.22; (△) 2.8, powder 0.23; (×) 3.0, powder 0.24.

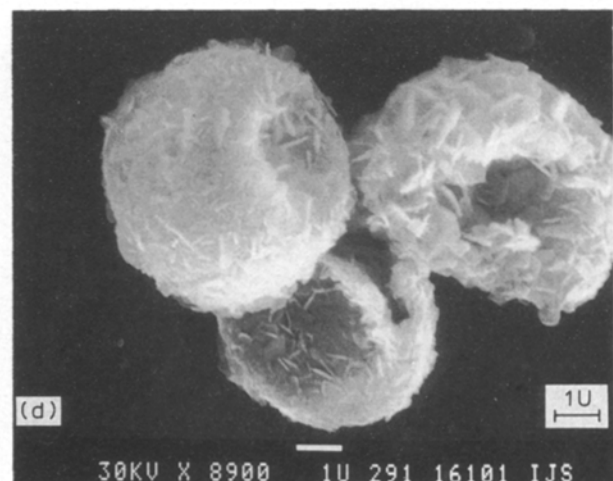
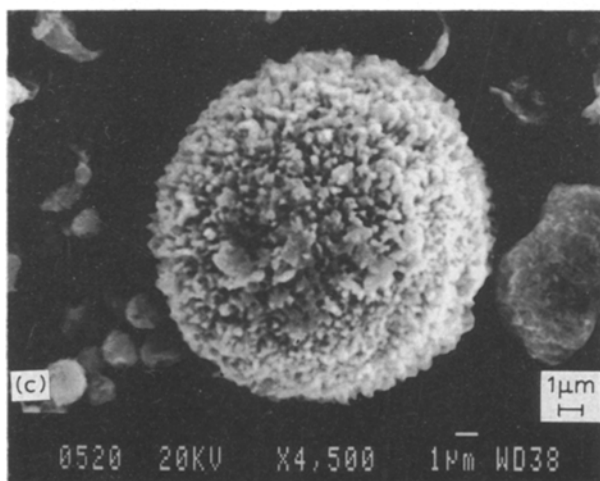
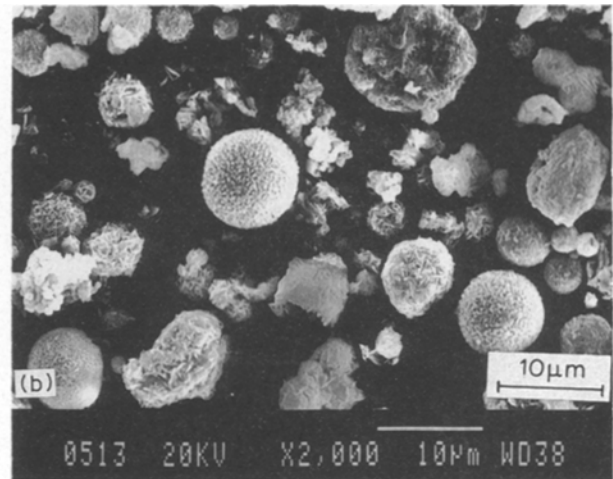
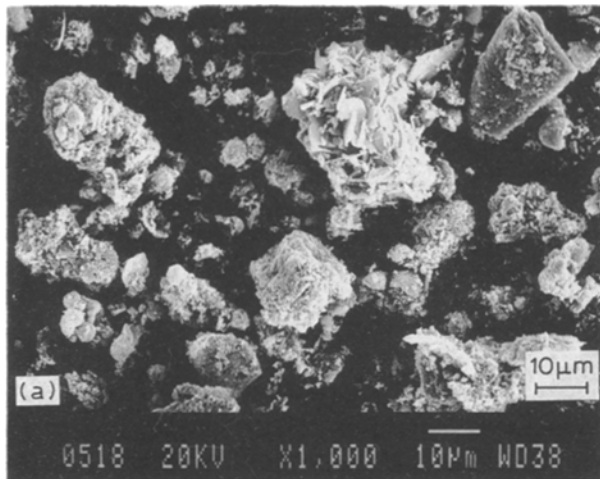


Figure 7 Scanning electron micrographs of $\text{Zn}(\text{NO}_3)_2 \cdot 6\text{H}_2\text{O}$ (a) decomposed conventionally at, 573 K and by means of the reaction spray process at (b) 1073 K and (c) 1173 K, respectively, and (d) for $\text{Zn}(\text{NO}_3)_2 \cdot 6\text{H}_2\text{O}$ + additives decomposed at 1173 K.

chromium, manganese, cobalt and nickel. Bismuth and antimony, which exist in the starting composition, are not identified. We believe that these particle inhomogeneities are the consequence of the nature of the feeding solution which was in the form of a suspension: i.e., in the first step of dilution of the melt mixture of crystallohydrate, hydrolysis occurred to some extent implying component inhomogeneities in the feeding solution, although being thoroughly mixed. These component inhomogeneities should persist in the final product which becomes a mixture of particles with some compositional inhomogeneities. Note that these particle inhomogeneities are not observed in the powder obtained by simple conventional thermal dehydration and decomposition in static conditions of the melt of crystallohydrate [16] where the composition of each examined particle is the same (Fig. 8b). From our previous results [19], bismuth is responsible for the formation and the height of the potential barrier in ZnO-based non-linear ceramics, while antimony is located in the form of $Zn_7Sb_2O_{12}$ spinel phase along

ZnO grain boundaries and has an influence on microstructure design.

3.3. Electrical properties

The non-linearity coefficient, α_2 , observed in the range from 10–100 $A\ m^{-2}$ for compacted and sintered samples of powder 0.24 realized its maximum values ($\alpha_2 \approx 30$) by sintering at 1473 K, while the non-linearity coefficients, α_1 , in the low-current region are relatively low, and the leakage current is about 40 $\mu A\ cm^{-2}$ for this sintering temperature (Table II). The values of the breakdown fields decreased from 1100 $V\ mm^{-1}$ at sintering temperature of 1373 K, to approximately 400 $V\ mm^{-1}$ at 1573 K. The relatively higher values of the breakdown fields, observed in this work, when compared to similar systems obtained by conventional dehydration and decomposition of the melt of crystallohydrates [16], could be the consequence of microstructure refinement due to the existence of very uniform and spherical particles when the

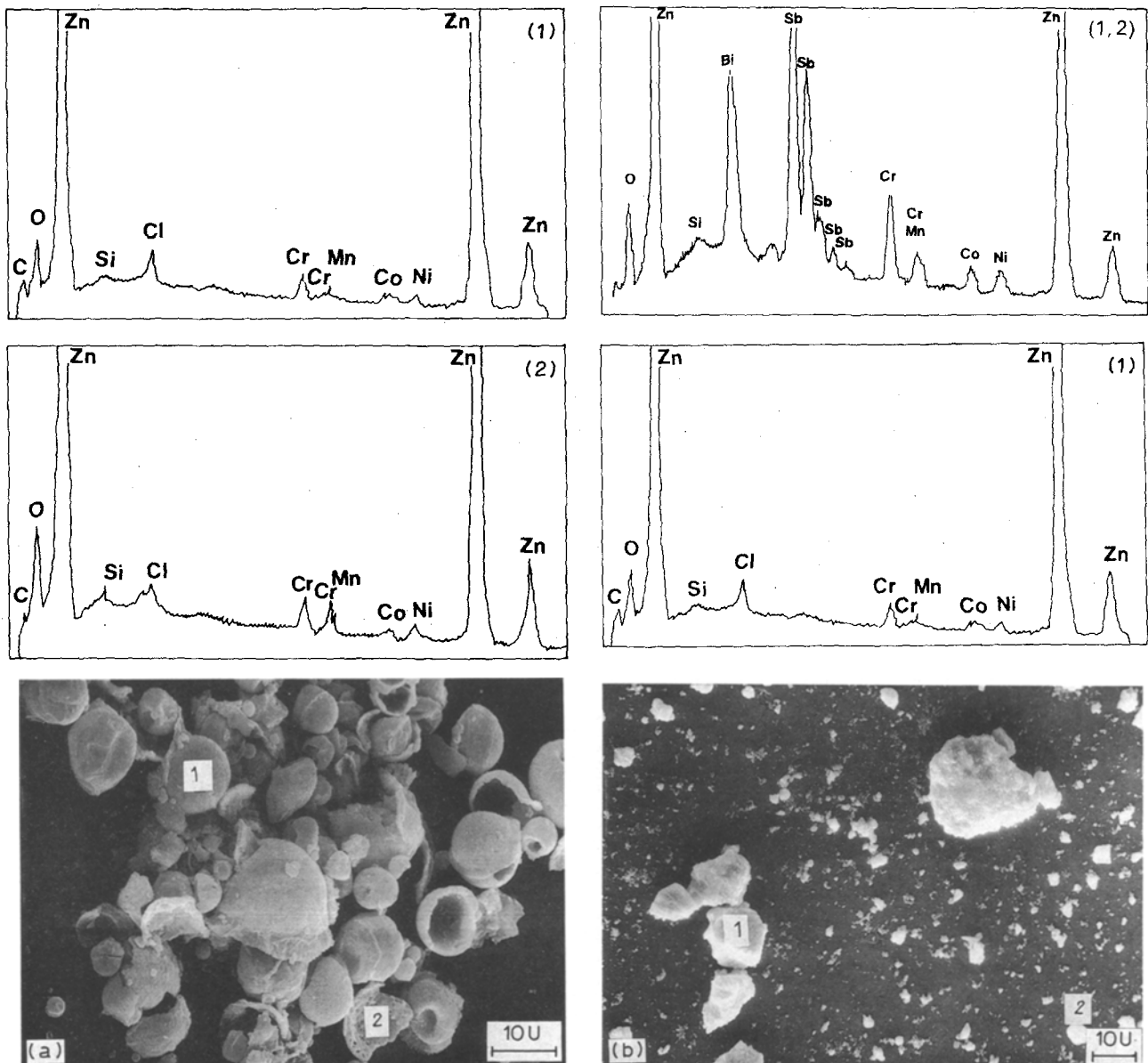


Figure 8 EDS analysis of the particle surface (1) and of the bulk (2) for powder 0.24 (a), as well as for the powder obtained by conventional dehydration and decomposition of the melt of crystallohydrates (1, 2) (b).

TABLE II Electrical properties of the samples sintered at 1473 K for the system obtained by means of the reaction spray process and for those obtained by conventional decomposition of the melts of crystallohydrates [16]

Electrical properties	Present work	[16]
α_1 ($1-10 \text{ A m}^{-2}$)	13	32
α_2 ($10-100 \text{ A m}^{-2}$)	30	27
J_L ($\mu\text{A cm}^{-2}$)	40	≤ 1
K_c (V mm^{-1})	760	380

powder preparation proceeds in the dispersion phase. Unfortunately, the expectation of a uniform component distribution in each particle when the powder is obtained by means of the reaction spray process is not realized, when EDS results are considered. Relatively high values of leakage currents and low values of the non-linearity coefficients in the low-current region ($1-10 \text{ A m}^{-2}$) are the consequence of non-uniform component distribution at the level of each particle. This compositional inhomogeneity in the powder is not originated by the reaction spray process, but by the nature of the solution, as mentioned above, and should be avoided by proper preparation of the initial feeding solution.

4. Conclusion

High-purity fine ceramic powders based on ZnO were prepared by the reaction spray process under various experimental conditions and characterized by means of DT/TG analysis, XRD, SEM, particle-size distribution and EDS.

The effect of the reaction spray process temperature on the phase content and the relative degree of decomposition was examined in the case of zinc nitrate solution as a model system. It was shown that the content of ZnO phase increased with increasing temperature of the reaction spray process. When hot gases flow over the as-prepared powder in the exhaust, the adsorption of water vapour is suppressed and the presence of an intermediate phase $\text{Zn}_5(\text{NO}_3)_2(\text{OH})_8 \cdot 2\text{H}_2\text{O}$ diminished.

The particles obtained are hollow spherical shells and shell fragments and seems to be an aggregate of small individual particles. The particle-size distribution is log-normal with an average particle size of about $3 \mu\text{m}$.

Varistor ceramics with the non-linearity coefficient $\alpha = 30$ and the breakdown voltage $K_c \approx 700 \text{ V mm}^{-1}$ were obtained by sintering of compacts of multicomponent powder with nominal composition $(100-X)\text{ZnO} + Y$ additives at 1473 K for 60 min. Further developments in obtaining homogeneous feeding solution, when a multicomponent system is required, will utilize the obvious advantageous of the reaction spray process in order to obtain uniform composition at the level of each particle. This will cause improvement in electrical properties.

Acknowledgements

This research was financially supported by the Republic Science Foundation through the project "Physicochemical Processes in Homogeneous and Heterogeneous Systems", and "Metal and Ceramics Matrix Composites" and partly by the National Institute for Standards and Technology, Gaithersburg, through funds made available to the US-Yugoslav Joint Board on Scientific and Technological Cooperation for the project "Synthesis and Microanalysis of Ceramics". In addition, the authors thank Mr M. Ignis for his contribution in furnace construction.

References

1. D. R. UHLMANN, B. J. J. ZELINSKI and G. E. WNEK, in "Better Ceramics Through Chemistry", edited by C. J. Brinker, D. E. Clark and D. R. Ulrich (Elsevier, 1984), pp. 59-70.
2. E. MATIJEVIĆ, *Ann. Rev. Mater. Sci.* **15** (1985) 483.
3. D. M. ROY, R. R. NEONGAONKAR, P. O. O'HOLLERAN and R. ROY, *Ceram. Bull.* **56** (1977) 1023.
4. M. J. RUTHNER, *J. Sci. Sintering* **6** (1/2) (1974) 81.
5. T. Q. LIU, O. SAKURAI, N. MIZUTANI and M. KATO, *J. Mater. Sci.* **21** (1986) 3698.
6. D. L. CHESS, C. A. CHESS and W. B. WHITE, *J. Amer. Ceram. Soc.* **66** (1983) C-205.
7. D. W. SPROSON, G. L. MESSING and T. J. GARDNER, *Ceram. Int.* **12** (1986) 3.
8. E. IVERS-TIFFEE and K. SEITZ, *Amer. Ceram. Soc. Bull.* **66** (1987) 1384.
9. N. TOHGE, M. TATSUMISAGO, T. MINAMI, K. OKUYAMA, K. ARAI, Y. INADA and Y. KOUSAKA, *J. Mater. Sci. Mater. Electron.* **1** (1990) 46.
10. S. S. JADA, *J. Mater. Sci. Lett.* **9** (1990) 565.
11. H. ISHIZAWA, O. SAKURAI, N. MIZUTANI and M. KATO, *Amer. Ceram. Soc. Bull.* **65** (1986) 1399.
12. B. DUBOIS, D. RUFFIER and P. ODIER, *J. Amer. Ceram. Soc.* **72** (1989) 713.
13. K. TAKIGAWA, K. NONAKA, K. OKADA and N. OTSUKA, *Brit. Ceram. Trans. J.* **89** (1990) 82.
14. R. J. SULLIVAN, T. T. SINIVASAN and R. E. NEWNHAM, *J. Amer. Ceram. Soc.* **73** (1990) 3715.
15. O. MILOŠEVIĆ, D. VASOVIĆ, D. POLETI, LJ. KARANOVIĆ, V. PETROVIĆ and D. USKOKOVIĆ, in "Science of Sintering: New Directions for Materials Processing and Microstructural Control", edited by D. P. Uskoković, H. Palmour III and R. M. Spriggs (Plenum Press, New York, London, 1989) pp. 117-26.
16. O. MILOŠEVIĆ, D. VASOVIĆ, D. POLETI, LJ. KARANOVIĆ, V. PETROVIĆ and D. USKOKOVIĆ, in "Ceramic Transactions", Vol. 3, edited by L. M. Levinson (The American Ceramic Society, Westerville, OH, 1989) pp. 395-402.
17. B. S. CHIOU, Y. J. TSAI and J. G. DUH, *J. Mater. Sci. Lett.* **7** (1988) 785.
18. T. J. GARDNER and G. L. MESSING, *Ceram. Bull.* **63** (1984) 1498.
19. O. MILOŠEVIĆ, D. VASOVIĆ, D. POLETI, LJ. KARANOVIĆ, V. PETROVIĆ and D. USKOKOVIĆ, in "Euro-Ceramics: Properties of Ceramics", Vol. 2, edited by G. de With, R. A. Terpstra and R. Metselaar, (Elsevier, 1989) 2382-87.

Received 12 February
and accepted 11 August 1992